

A Kinetic Study of the Reaction of OH with Xylenes Using the Relative Rate/Discharge Flow/Mass Spectrometry Technique

Deepali Mehta, Andrew Nguyen, Anthony Montenegro, and Zhuangjie Li*

Department of Chemistry and Biochemistry, California State University—Fullerton, Fullerton, California 92834

Received: May 29, 2009; Revised Manuscript Received: September 22, 2009

A kinetics study for the reaction of OH with *o*-, *m*-, and *p*-xylene has been conducted at 1–10 Torr and 240–340 K using the relative rate/discharge flow/mass spectrometry technique with 1,4-dioxane as the reference compound. At 298 K, the rate constants for the reaction of OH with all three isomers of xylene exhibited prominent positive pressure dependence up to 5 Torr, and the reactions reached a high-pressure limit at 8 Torr, with a high pressure limit rate constant of $k_{o\text{-xylene}} = (1.19 \pm 0.07) \times 10^{-11} \text{ cm}^3 \text{ molecule}^{-1} \text{ s}^{-1}$, $k_{m\text{-xylene}} = (2.14 \pm 0.14) \times 10^{-11} \text{ cm}^3 \text{ molecule}^{-1} \text{ s}^{-1}$, and $k_{p\text{-xylene}} = (1.19 \pm 0.07) \times 10^{-11} \text{ cm}^3 \text{ molecule}^{-1} \text{ s}^{-1}$, respectively, which are in good agreement with literature values. The results of the temperature-dependence study indicated that, in all three reactions, there is negative temperature dependence at temperatures greater than 298 K. The reaction of OH with xylene may proceed with addition of the OH radical to the benzene ring at room temperature and below, with an equilibrium established between the reactants and the xylene–OH adduct. At 298–340 K, the equilibrium is shifted toward the reactants, giving rise to a negative temperature dependence of the rate constant, and this may also associate with a transition of the reaction from the addition mechanism to the abstraction mechanism. On the basis of our kinetic results at 277 K, the atmospheric lifetimes of *o*-, *m*-, and *p*-xylene are estimated to be about 29, 14, and 31 h, respectively.

Introduction

The three members of the xylene isomer family, *o*-, *m*- and *p*-xylene, are air pollutants emitted into the atmosphere from anthropogenic sources such as gasoline, diesel fuels, kerosene, and marine paints.^{1,2} The atmospheric concentration of *o*-, *m*-, and *p*-xylene in the United States has been reported to be in the range of 18–370, 27–550, and 15–270 ppt, respectively.^{3–5} Exposure to high concentrations (ppm) of xylene is known to significantly affect human health and the environment.⁶ Adverse health effects related to direct xylene exposure include nausea, ocular and mucus tract irritation, and the disturbance of the central nervous system.⁶ The atmospheric oxidation of xylene contributes to the production of photochemical smog.⁷ A recent study has also indicated that the atmospheric degradation of xylene can lead to the formation of secondary organic aerosols.⁸

Xylene is removed from the atmosphere via reactions with Cl, NO₃, and OH radicals,⁷ with the primary removal process initiated via reaction with OH.⁹ The kinetics of the reaction of xylene with OH is therefore important in assessing the contribution of these compounds to the air pollution system.

Over the last several decades, many groups have studied the kinetics of the reaction of xylene with the hydroxyl radical.^{9–22} During the 1970s, the reaction of xylene with OH was studied using techniques such as relative rate/discharge photolysis/UV-vis, flash photolysis, and flash photolysis/resonance fluorescence, with rate constants reported to be $k_{o\text{-xylene}} = (1.28–1.53) \times 10^{-11} \text{ cm}^3 \text{ molecule}^{-1} \text{ s}^{-1}$, $k_{m\text{-xylene}} = (1.94–2.40) \times 10^{-11} \text{ cm}^3 \text{ molecule}^{-1} \text{ s}^{-1}$, and $k_{p\text{-xylene}} = (1.01–1.53) \times 10^{-11} \text{ cm}^3 \text{ molecule}^{-1} \text{ s}^{-1}$, respectively.^{12,14,18,19} Using various techniques in the 1980s, research groups reported rate constants of $k_{o\text{-xylene}} = (1.22–1.42) \times 10^{-11} \text{ cm}^3 \text{ molecule}^{-1} \text{ s}^{-1}$, $k_{m\text{-xylene}} = (1.86–2.54) \times 10^{-11} \text{ cm}^3 \text{ molecule}^{-1} \text{ s}^{-1}$, and $k_{p\text{-xylene}} =$

$(1.25–1.36) \times 10^{-11} \text{ cm}^3 \text{ molecule}^{-1} \text{ s}^{-1}$ for the xylene + OH system.^{9,11,13,15–17,21} In the 1990s, the discharge photolysis technique was used to study the reaction of OH with *m*-xylene, and rate constants in the range of $(2.06–2.45) \times 10^{-11} \text{ cm}^3 \text{ molecule}^{-1} \text{ s}^{-1}$ were observed.^{20,22} At the turn of the century, the reaction of *o*-xylene with OH was studied using the relative rate/gas chromatography/mass spectrometry technique, with a rate constant of $k_{o\text{-xylene}} = (1.14 \pm 0.03) \times 10^{-11} \text{ cm}^3 \text{ molecule}^{-1} \text{ s}^{-1}$ being reported.¹⁰ Despite these extensive studies, previous kinetic investigations of these reactions have mainly been conducted at room temperature and high pressure conditions.

There were only a couple of temperature dependence kinetics studies for the reaction of xylene with OH radicals.^{16,18} For all three xylene isomers, the temperature dependence of the rate constants has been studied at 296–473 K by Perry et al. and at 298–970 K by Nicovich et al. Nicovich et al. has also studied the *m*-xylene + OH system at 250 and 269 K. The limited temperature dependence kinetics investigations for the reaction of OH with xylene suggest that further kinetics studies are needed, especially at temperatures that are representative of the troposphere, which can better facilitate atmospheric composition modeling.

Kinetics data revealing the pressure dependence of *o*-, *m*-, and *p*-xylene + OH reaction also are needed to understand the reaction mechanism of the xylene + OH system. To date, there has only been one pressure dependence study.¹⁹ Ravishankara et al. examined the kinetics of the xylene + OH reaction in a pressure range of 3–200 Torr, and they reported that there is no pressure dependence at pressures higher than 20 Torr based on the statistically insignificant variation in the rate constants at 20 and 200 Torr, with both helium and argon as a diluent gas.¹⁹ On the basis of their kinetic results at 3 Torr, they concluded that the high-pressure limit for the OH + xylene system lies between 3 and 20 Torr and that the exact high-pressure limit for these reactions remains to be determined.

* Corresponding author. Phone: (657) 278-3585. Fax: (657) 626-8010. E-mail: zli@fullerton.edu.

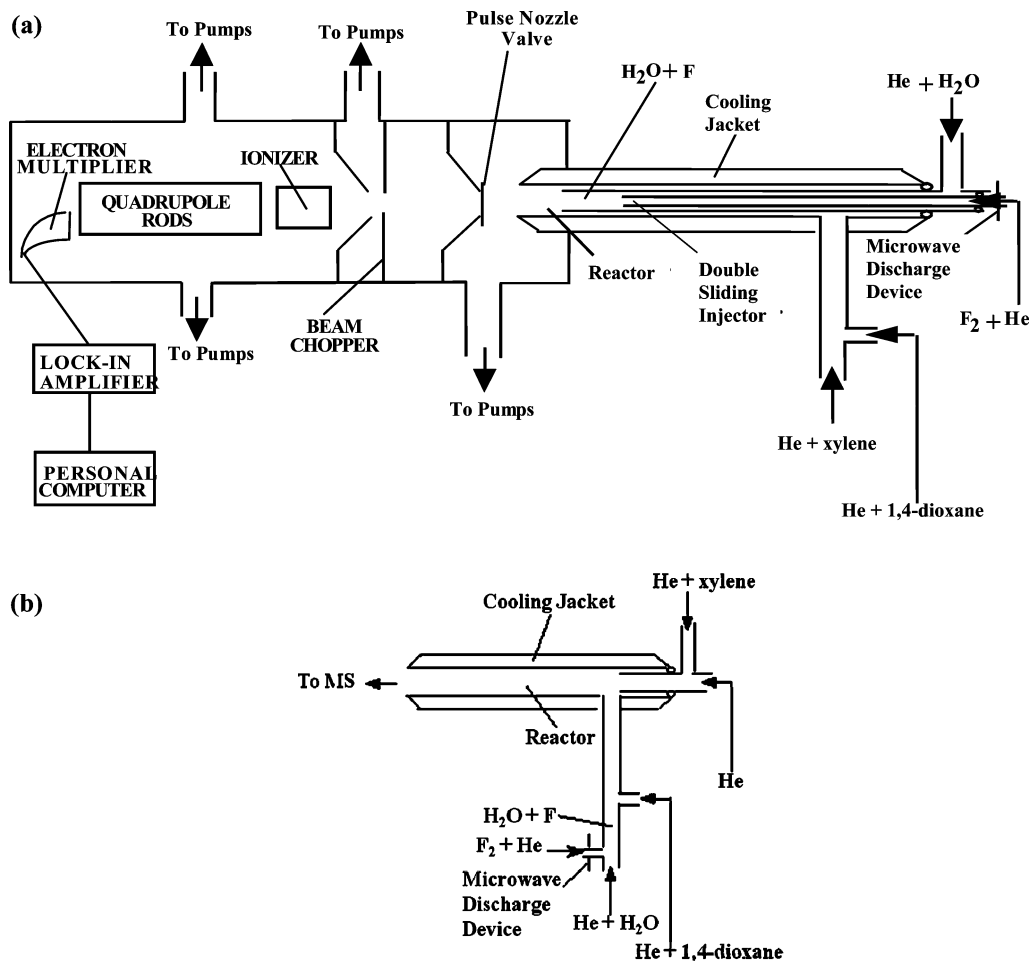


Figure 1. Schematic of the relative rate/discharge flow/mass spectrometry apparatus.

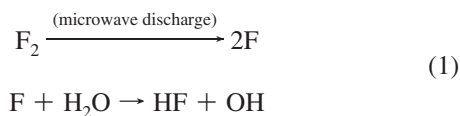
The present work aims to enhance the existing kinetics database by performing a kinetics study of the reaction of *o*-, *m*-, and *p*-xylene with the hydroxyl radical at 1–10 Torr and 240–340 K using the relative rate/discharge flow/mass spectrometry (RR/DF/MS) technique that has been recently developed in our laboratory.²³ We have focused on the investigation of the pressure dependence from 1–10 Torr to pinpoint the high-pressure limits for these reactions. We also determined the rate constants for these reactions at various temperatures, including temperatures that are representative of the troposphere. These pressure- and temperature-dependent kinetics studies will allow us to gain insight into the mechanism of this reaction at a fundamental level and estimate the lifetime of *o*-, *m*-, and *p*-xylene in the atmosphere.

Experimental Section

The RR/DF/MS technique has been previously utilized by our group to study the reaction of VOCs with OH at various temperatures and pressures.^{23,26–29} Figure 1 shows the RR/DF/MS experimental apparatus, with Figure 1a describing the arrangement of the kinetics investigation and Figure 1b presenting the setup of controlled experiments for secondary reaction checks.

The OH radicals were generated in situ by reacting F atoms with H₂O inside a double-sliding injector consisting of two concentric Pyrex tubes with internal diameters of 7 and 12.7 mm, respectively. Halocarbon wax (series 1500, Halocarbon Products Corp.) was coated on the internal surface of the inner Pyrex tube to reduce the loss of F atoms via reacting with SiO₂.

Water vapor was carried by 100 sccm (standard cubic centimeter per minute) of helium to the double-sliding injector, and the fluorine atoms were generated by microwave discharging (Ophos Instruments, Inc., model MPG-4) 5% F₂ that was carried by 1500 sccm of helium, resulting in the following reactions for OH production within the sliding injector:



Xylene and 1,4-dioxane were carried by 200 sccm of helium each and were mixed prior to entering the reactor through a side arm inlet to ensure that they shared the same reaction time with the OH radicals.

The flow reactor consisted of an 80 cm long Pyrex tube with an internal diameter of 5.08 cm. The internal surface of the reactor was covered with a 0.79 mm thick poly(tetrafluoroethylene) (TFE) Teflon sheet to reduce the wall loss of OH radicals and minimize the deposition of reaction products on the inner wall of the reactor, preventing contamination of the flow reactor. The temperature of the reactor was varied by circulating a heating/cooling fluid (Neslab ULT-80) through a Pyrex jacket surrounding the flow tube. Methanol was used as coolant for kinetics investigation at temperatures below 298 K, and water was used as heating medium for reactor temperatures at and above 298 K. An

Edwards E2M175 mechanical pump was used to maintain a total pressure of 1–10 Torr in the flow tube and a steady-state gas flow with a mean gas flow velocity of approximately 1200 cm s⁻¹ in the flow reactor. The interaction between OH radicals and the VOCs was confined to a contact distance of 30 cm, corresponding to a reaction time of 24 ms. A removable liquid nitrogen trap was placed downstream of the reactor to protect the vacuum pump from corrosive reactants and products. An electron impact mass spectrometer (Extrel MAX-1000) for the monitoring of reactants was housed in a vacuum chamber, which was two-stage differentially pumped using two 6-in. diffusion pumps with liquid nitrogen baffles. The ultimate vacuum was less than 5 × 10⁻¹⁰ Torr in the second stage.

Mass spectrometric detection of reactants was carried out by continuous sampling at the downstream end of the flow tube. A 200-Hz tuning fork chopper was used for beam modulation. Ion signals were sent to a SR510 lock-in amplifier that was referenced to the chopper frequency. The amplified analog signal was converted to digital form using an analog to digital convertor (Analog Devices RTI/815) and recorded on a micro-computer. An electron impact energy of 40 eV was used in order to minimize fragmentation of the reactants while maximizing the ionization efficiency. Parent ions of xylene and 1,4-dioxane were monitored at *m/z* = 106 and 88, respectively. No significant fragment ions were observed at *m/z* = 88 from xylene nor from the xylene + OH product. This suggested that there was very little overlap in the mass spectroscopic detection of both target and reference compounds so that the decay of both xylene and 1,4-dioxane could be monitored simultaneously without interference from other species. Under normal operational conditions, the detection limit of gas samples was on the order of 10⁹–10¹⁰ molecules cm⁻³, depending on the individual species detected.

The VOCs were quantified by calibrating the mass spectral signal using known concentrations of the VOCs.^{23,26–29} The calibration was performed by either introducing a known amount of a VOC sample into the reactor or by quantitative conversion of the species through chemical reactions. The initial concentration of the OH radicals was taken to be the same as the atomic fluorine concentration, which was found by measuring the [F₂] difference between “switch on” and “switch off” of the microwave discharge device while F₂ was passed through the discharge cavity, i.e. [F] = 2 × Δ[F₂] = 2 × ([F₂]_{switch off} – [F₂]_{switch on}). It was determined that ≥96% of the F₂ dissociated under 50 W of microwave discharge power, with dissociation efficiency being inversely proportional to the amount of F₂. An excessive amount of water (~7 × 10¹⁴ molecules cm⁻³) was introduced into the double-sliding injector to ensure complete titration of the fluorine atoms in the present work. The OH radical concentration was varied by adjusting the amount of F₂ [(0–2) × 10¹³ molecules cm⁻³] passing through the microwave discharge cavity. The stoichiometric consumption of the VOCs by the OH radicals was then used to determine the concentration of the VOCs in the flow reactor, and the intensity of the mass spectral signal was found to be always linearly proportional to the amount of organic samples in the reactor.^{23,26–29}

Experiments were performed at a given temperature and pressure for two or more trials on different days under the same experimental condition so that the consistency of the experimental results could be verified. For the kinetics investigation as a function of pressure, the total pressure of the reactor was regulated at 1–10 Torr by adjusting a throttle valve located at the downstream of the vacuum line.

In the present study, the experimental data were analyzed on the basis of the RR/DF/MS formulation.²³ The RR/DF/MS technique is based on the competition of the target (xylene) and reference (1,4-dioxane) reactions with OH radicals in the reactor:



Assuming that both xylene and 1,4-dioxane react only with OH, it can be shown that²³

$$\ln\left(\frac{[\text{xylene}]_{t,[\text{OH}]=0}}{[\text{xylene}]_{t,[\text{OH}]}}\right) = \frac{k_{\text{xylene}}}{k_{1,4\text{-dioxane}}}\ln\left(\frac{[1,4\text{-dioxane}]_{t,[\text{OH}]=0}}{[1,4\text{-dioxane}]_{t,[\text{OH}]}}\right) \quad (\text{I})$$

where [xylene]_{*t*,[OH]=0} and [1,4-dioxane]_{*t*,[OH]=0} represent the concentration of xylene and 1,4-dioxane in the absence of OH radicals at time *t*, [xylene]_{*t*,[OH]} and [1,4-dioxane]_{*t*,[OH]} represent the concentration of xylene and 1,4-dioxane in the presence of OH radicals at time *t*, and *k*_{xylene} and *k*_{1,4-dioxane} are the rate constants for reactions 2 and 3, respectively. By plotting ln([xylene]_{*t*,[OH]=0}/[xylene]_{*t*,[OH]}) vs ln([1,4-dioxane]_{*t*,[OH]=0}/[1,4-dioxane]_{*t*,[OH]}), a straight line is expected with a slope representing *k*_{xylene}/*k*_{1,4-dioxane}. Multiplying the slope by *k*_{1,4-dioxane}, whose value is known at given temperatures, results in *k*_{xylene}. Repeating the same procedure at various pressures and temperatures allows for a pressure- and temperature-dependence study for the kinetic parameters of reaction 2.

The lifetime of xylene in the atmosphere is estimated using the following relationship

$$\tau_{\text{xylene}} \approx \frac{1}{k_{\text{xylene}+\text{OH}}[\text{OH}]} \quad (\text{II})$$

where *k*_{xylene+OH} represents the rate constant for the reaction of xylene with OH at a particular pressure and temperature, and [OH] represents the average concentration of OH in the troposphere.

Ultra-high-purity helium (99.999%) was obtained from Oxygen Service Co., and F₂ (5% in He) was obtained from Spectra Gases Inc. 1,4-Dioxane (>99%) was obtained from Fisher Scientific, *o*-xylene from EMD, *m*-xylene from Baker (Baker grade), and *p*-xylene from Acros (99%). All these chemicals were used as received. Deionized water was used as an OH precursor.

Results and Discussion

It was observed in the present work that both xylene and 1,4-dioxane reacted with F₂ molecules at higher pressures, causing decay of these compounds. To reduce this effect, the microwave discharge was kept “on” to minimize the direct contact between reactants and F₂ during data collection. It was that estimated under such experimental conditions less than 1% of the reactants decay can be attributed to the reaction of the reactants with nondissociated F₂.

Typical kinetic data for the reaction of *o*-, *m*-, and *p*-xylene with OH at 1 Torr and 298 K is presented in Figure 2, in which the target and reference compounds are depleted by approximately 0–50% of their original concentration. Our data indicate that, within that range, the decay of the reactants can be well-described by eq I. Fitting all of the data points using linear regression yielded a straight line with a slope

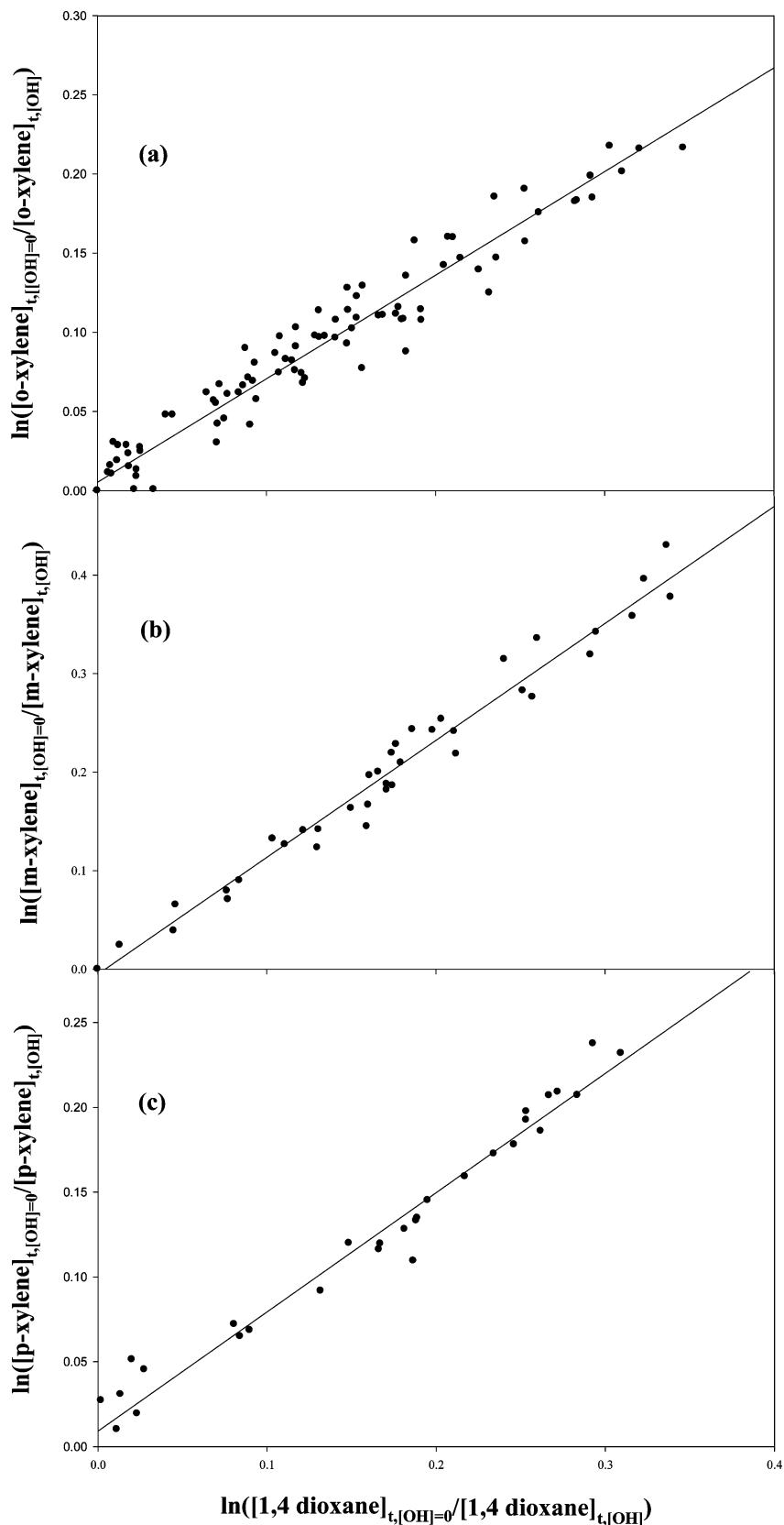


Figure 2. Typical kinetic data of (a) *o*-xylene + OH, (b) *m*-xylene + OH, and (c) *p*-xylene + OH at 1 Torr and 298 K, using 1,4-dioxane as a reference compound. The reactant initial concentrations are in the range of $(0.6\text{--}1.0) \times 10^{14}$, $(0.8\text{--}1.3) \times 10^{14}$, $(0\text{--}4.0) \times 10^{13}$ molecules cm^3 for xylenes, 1,4-dioxane, and OH, respectively.

of $k_{o\text{-xylene}}/k_{1,4\text{-dioxane}} = 0.654 \pm 0.037$, $k_{m\text{-xylene}}/k_{1,4\text{-dioxane}} = 1.16 \pm 0.05$, and $k_{p\text{-xylene}}/k_{1,4\text{-dioxane}} = 0.703 \pm 0.037$, respectively. Using the recommended rate constant of $k_{1,4\text{-dioxane}} = (1.09 \pm$

$0.05) \times 10^{-11}$ cm^3 molecule $^{-1}$ s $^{-1}$ for the reaction of 1,4-dioxane with OH,²⁴ the rate constants for the reaction of xylene with OH were determined to be $k_{o\text{-xylene}} = (0.713 \pm$

TABLE 1: Rate Constants of the Reaction of Xylene with OH at Various Pressures and Room Temperature

P_{total} (Torr)	reference compound	slope ($k_{\text{xylene}}/k_{1,4\text{-dioxane}}$)	$k \times 10^{11}{}^a$ ($\text{cm}^3 \text{ molecule}^{-1} \text{ s}^{-1}$)	technique ^d	ref
<i>o</i> -Xylene					
1.0–1.1	1,4-dioxane	0.654 ± 0.037	0.713 ± 0.052 (101)	RR/DF/MS	this work
3.0–3.1	1,4-dioxane	0.872 ± 0.060	0.951 ± 0.078 (44)	RR/DF/MS	this work
5.0–5.1	1,4-dioxane	1.04 ± 0.04	1.13 ± 0.07 (52)	RR/DF/MS	this work
8.0–8.1	1,4-dioxane	1.09 ± 0.03	1.19 ± 0.07 (106)	RR/DF/MS	this work
9.0–9.1	1,4-dioxane	1.05 ± 0.09	1.14 ± 0.11 (22)	RR/DF/MS	this work
20 ^b			1.29 ± 0.38	FP/RF	19
20 ^c			1.30 ± 0.03	FP/RF	19
200 ^b			1.24 ± 0.01	FP/RF	19
<i>m</i> -Xylene					
1.0–1.1	1,4-dioxane	1.19 ± 0.06	1.29 ± 0.09 (41)	RR/DF/MS	this work
3.0–3.1	1,4-dioxane	1.47 ± 0.05	1.60 ± 0.09 (37)	RR/DF/MS	this work
3 ^c			1.56 ± 0.14	FP/RF	19
5.0–5.1	1,4-dioxane	1.94 ± 0.07	2.12 ± 0.12 (60)	RR/DF/MS	this work
8.0–8.1	1,4-dioxane	1.96 ± 0.09	2.14 ± 0.14 (93)	RR/DF/MS	this work
9.0–9.1	1,4-dioxane	2.34 ± 0.29	2.55 ± 0.33 (21)	RR/DF/MS	this work
20 ^c			1.94 ± 0.08	FP/RF	19
20 ^b			2.14 ± 0.02	FP/RF	19
200 ^c			2.03 ± 0.19	FP/RF	19
200 ^b			2.06 ± 0.13	FP/RF	19
<i>p</i> -Xylene					
1.0–1.1	1,4-dioxane	0.703 ± 0.037	0.766 ± 0.053 (34)	RR/DF/MS	this work
3.0–3.1	1,4-dioxane	0.981 ± 0.060	1.07 ± 0.08 (28)	RR/DF/MS	this work
3 ^c			0.88 ± 0.12	FP/RF	19
5.0–5.1	1,4-dioxane	1.09 ± 0.04	1.19 ± 0.07 (67)	RR/DF/MS	this work
8.0–8.1	1,4-dioxane	1.09 ± 0.03	1.19 ± 0.07 (118)	RR/DF/MS	this work
9.0–9.1	1,4-dioxane	1.13 ± 0.09	1.23 ± 0.11 (26)	RR/DF/MS	this work
20 ^b			1.01 ± 0.10	FP/RF	19
200 ^b			1.05 ± 0.06	FP/RF	19

^a The number in parentheses represents the number of data points taken. Error bars are taken as 2σ . ^b He was used as a carrier bath gas. ^c Ar was used as a carrier bath gas. ^d DF, discharge flow; DP, direct photolysis; FP, flash photolysis; GC, gas chromatography; MS, mass spectrometry; RF, resonance fluorescence; RR, relative rate.

$0.052) \times 10^{-11} \text{ cm}^3 \text{ molecule}^{-1} \text{ s}^{-1}$, $k_{m\text{-xylene}} = (1.29 \pm 0.08) \times 10^{-11} \text{ cm}^3 \text{ molecule}^{-1} \text{ s}^{-1}$, and $k_{p\text{-xylene}} = (0.766 \pm 0.053) \times 10^{-11} \text{ cm}^3 \text{ molecule}^{-1} \text{ s}^{-1}$, respectively. The error bars associated with the values were taken as 2σ to account for experimental uncertainties such as scattering of the data and the fluctuation in pressure, temperature, incomplete F_2 dissociation, and flow rate during data acquisition. The error bar has also taken the errors in the reference rate constant into account.

Since the primary assumption of the RR/DF/MS technique is that the xylene and 1,4-dioxane reactants are dominantly consumed by OH, it is imperative to examine the possible contribution of secondary reactions to the decay of the reactants.^{23,26–29} In order to assess the effects of secondary reactions on the concentration of the target and reference reactants within the flow reactor, controlled experiments were carried out. In one controlled experiment, the effect of the products from 1,4-dioxane + OH on the decay of the xylene reactants was investigated by allowing the product to interact with each xylene isomer. Similarly, the effects of the xylene + OH products upon the decay of 1,4-dioxane were also examined by reconfiguring the experimental setup.

The setup for the controlled experiments is presented in Figure 1b. The OH radicals were reacted with a reactant (xylene or 1,4-dioxane) prior to entering the reactor through the side arm. The primary products were then allowed to enter the reactor to interact with another reactant (1,4-dioxane or xylene). It was found that the products from OH + xylene had little effect on the signal intensity of 1,4-dioxane (with an average error of 3%) and that the products from 1,4-dioxane + OH had little effect on the signal intensity of

xylene (with an average error of 2%), which suggest that these secondary reactions have insignificant effects on the kinetics results.

The reactions of xylene and 1,4-dioxane with O and H atoms that are generated from other secondary reactions could also potentially affect the decay of xylene and 1,4-dioxane and hence the accuracy of our kinetic results. These potential effects were assessed using chemical modeling employing the Runge–Kutta method for solving a system of coupled differential equations previously described in our work.^{23,26–29} With initial concentrations of 9.0×10^{13} , 1.3×10^{14} , and $4.0 \times 10^{13} \text{ molecules cm}^{-3}$ for xylene, 1,4-dioxane, and OH, our simulation results indicated that the O and H atom caused less than 1% decay in both reactants during 50 ms of reaction time. Since our kinetic data were collected within 24 ms of reaction time during the experiments, the kinetic results should be essentially free of the effects due to secondary reactions involving H and O atoms and therefore considered reliable.

A. Pressure Dependence of Xylene + OH. The pressure dependence of the rate constant for the reaction of xylene with OH at room temperature (298 K) is presented in Table 1 and Figure 3. The rate constants of the reactions of *o*-, *m*-, and *p*-xylene with OH all exhibit a prominent positive pressure dependence at 1–5 Torr and reach high pressure limit values at about 8 Torr, with a high pressure limit rate constants of $k_{o\text{-xylene}} = (1.19 \pm 0.07) \times 10^{-11} \text{ cm}^3 \text{ molecule}^{-1} \text{ s}^{-1}$, $k_{m\text{-xylene}} = (2.14 \pm 0.14) \times 10^{-11} \text{ cm}^3 \text{ molecule}^{-1} \text{ s}^{-1}$, and $k_{p\text{-xylene}} = (1.19 \pm 0.07) \times 10^{-11} \text{ cm}^3 \text{ molecule}^{-1} \text{ s}^{-1}$, respectively. The positive pressure dependence of these reactions suggests that the reaction of OH with *o*-, *m*-, and

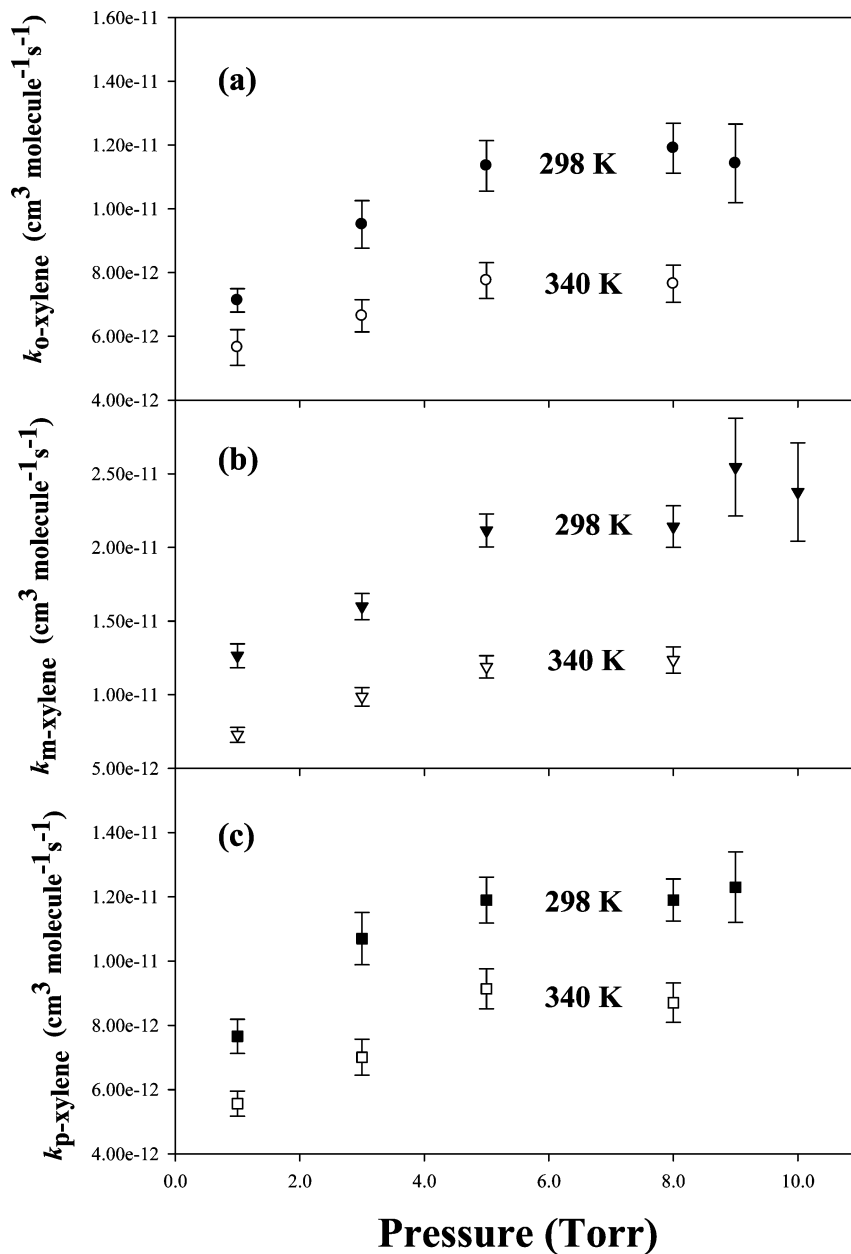


Figure 3. Rate constants of (a) *o*-xylene + OH, (b) *m*-xylene + OH, and (c) *p*-xylene + OH as a function of pressure at 298 K (filled data) and 340 K (unfilled data), respectively.

p-xylene proceeds via an addition mechanism at room temperature. Since the high pressure limit rate constants are desirable for atmospheric composition modeling, the study of temperature dependence of the rate constant for the reaction of xylene with OH radicals was conducted at 8 Torr in the present work.

B. Temperature Dependence of Xylene + OH. The results of the kinetics study for the reaction of xylene with OH at 240–340 K and 8 Torr are presented in Tables 2–4 and Figures 3 and 4. Within experimental uncertainty, our room temperature rate constants for the reaction of xylene with OH are in agreement with most previous literature values measured using different techniques.^{9–22} For *o*-xylene, our $k_{o\text{-xylene}}$ value only differs from the value of $k_{o\text{-xylene}} = (1.53 \pm 0.15) \times 10^{-11} \text{ cm}^3 \text{ molecule}^{-1} \text{ s}^{-1}$ reported by Hansen et al. by about 22% (see Table 2).¹⁴ In the case of *m*-xylene, our $k_{m\text{-xylene}}$ value is in excellent agreement with all previous measurements except that of $k_{m\text{-xylene}} = (1.94 \pm 0.08) \times 10^{-11} \text{ cm}^3 \text{ molecule}^{-1} \text{ s}^{-1}$ reported by Cox et al. (see Table 3).¹¹

Our room temperature rate constant for the reaction of *p*-xylene with OH is also in reasonably good agreement with other literature values except that of $k_{p\text{-xylene}} = (1.53 \pm 0.17) \times 10^{-11} \text{ cm}^3 \text{ molecule}^{-1} \text{ s}^{-1}$ reported by Perry et al. (Table 4).¹⁸ The reasons for the difference between our rate constant values and that reported by Hansen et al., Cox et al., and Perry et al. are not clear. For the rate constants determined using the relative rate technique, the use of different reference compounds might attribute to the discrepancy between our values and that of Cox et al. Nevertheless, it is interesting to observe that the *m*-xylene reacts with OH faster than the *o*- and *p*-isomers. It has been suggested that the meta-substituted isomer of xylene reacts quicker with OH than *o*- and *p*-xylene because meta-substitution enhances electrophilic addition of OH.¹⁶ This would be expected since meta substitution of xylene leads to the formation of a resonance-stabilized tertiary radical addition product. Our kinetics results seem to support this hypothesis. But further studies,

TABLE 2: Rate Constants of the Reaction of *o*-Xylene with OH at 240–340 K

<i>T</i> (K)	reference compound	$k_{o\text{-xylene}} \times 10^{11}$ ^a (cm ³ molecule ⁻¹ s ⁻¹)	<i>P</i> _{total} (Torr)	technique ^c	ref
240	1,4-dioxane	1.25 ± 0.09 (31)	8.0–8.1	RR/DF/MS	this work
260	1,4-dioxane	1.20 ± 0.09 (35)	8.0–8.1	RR/DF/MS	this work
277	1,4-dioxane	1.19 ± 0.08 (23)	8.0–8.1	RR/DF/MS	this work
295	toluene	1.14 ± 0.03	760	RR/GC/MS	10
296	propene	1.22 ± 0.19	735	RR/FP/GC	9
297	cyclohexane	1.24	758	RR/DP/GC	13
298	1,4-dioxane	1.19 ± 0.07 (106)	8.0–8.1 ^b	RR/DF/MS	this work
298	ethylene	1.33	758	RR/SP/GC	11
298		1.53 ± 0.15	101	FP/RF	14
298		1.42 ± 0.17	99.8	FP/RF	16
298	<i>n</i> -hexane	1.32 ± 0.06	760	RR/DP/GC	17
298		1.43 ± 0.15	100	FP/RF	18
298		1.24 ± 0.01	200 ^b	FP/RF	19
300		1.3	760	DP/GC	15
304	<i>n</i> -butane	1.28 ± 0.38	758	RR/DP/UV-vis	12
320	1,4-dioxane	0.965 ± 0.083 (23)	8.0–8.1	RR/DF/MS	this work
320		1.58 ± 0.18	99.8	FP/RF	16
340	1,4-dioxane	0.786 ± 0.068 (21)	8.0–8.1	RR/DF/MS	this work
340	1,4-dioxane	0.775 ± 0.056 (18)	4.9–5.0	RR/DF/MS	this work
340	1,4-dioxane	0.664 ± 0.051 (17)	3.0–3.1	RR/DF/MS	this work
340	1,4-dioxane	0.5650 ± 0.056 (14)	1.03–1.04	RR/DF/MS	this work

^a The number in parentheses represents the number of data points taken. Error bars are taken as 2σ . ^b He was used as a carrier bath gas. ^c DF, discharge flow; DP, direct photolysis; FP, flash photolysis; GC, gas chromatography; MS, mass spectrometry; RF, resonance fluorescence; RR, relative rate; SP, sensitized photolysis; UV-vis, ultraviolet-visible spectroscopy.

TABLE 3: Rate Constants of the Reaction of *meta*-Xylene with OH at 240–340 K

<i>T</i> (K)	reference compound	$k_{m\text{-xylene}} \times 10^{-11}$ ^a (cm ³ molecule ⁻¹ s ⁻¹)	<i>P</i> _{total} (Torr)	technique ^d	ref
240	1,4-dioxane	2.76 ± 0.20 (35)	8.0–8.1	RR/DF/MS	this work
250		2.65 ± 0.25	100	FP/RF	16
260	1,4-dioxane	2.76 ± 0.26 (20)	8.0–8.1	RR/DF/MS	this work
269		2.56 ± 0.43	100	FP/RF	16
277	1,4-dioxane	2.46 ± 0.18 (35)	8.0–8.1	RR/DF/MS	this work
296	cyclohexane	2.09 ± 0.146	740	RR/DP/GC	20
296		2.30 ± 0.35	735	RR/FP/GC	9
296	butadiene	2.06 ± 0.006	758	RR/DP/GC	22
296	<i>trans</i> -2-butene	2.17 ± 0.02	758	RR/DP/GC	22
296	trimethylbenzene	2.18 ± 0.004	758	RR/DP/GC	22
296	di- <i>n</i> -butyl ether	2.14 ± 0.01	758	RR/DP/GC	22
296	propene	2.15 ± 0.04	758	RR/DP/GC	22
296	methylcyclohexane	2.45 ± 0.02	758	RR/DP/GC	22
296	<i>n</i> -nonane	2.13 ± 0.02	758	RR/DP/GC	22
296	cyclohexane	2.33 ± 0.04	758	RR/DP/GC	22
296	toluene	2.29 ± 0.03	758	RR/DP/GC	22
296	cyclopentane	2.34 ± 0.04	758	RR/DP/GC	22
297	cyclohexane	2.27	757	RR/DP/GC	13
297		2.36 ± 0.24	100	FP/RF	14
298	1,4-dioxane	2.14 ± 0.14 (93)	8.0–8.1 ^b	RR/DF/MS	this work
298	ethylene	1.86	758	RR/SP/GC	11
298		2.54 ± 0.35	100	FP/RF	16
298		2.34 ± 0.0697	757	RR/DP/GC	17
298		2.03 ± 0.19	200 ^c	FP/RF	19
298		2.06 ± 0.13	200 ^b	FP/RF	19
298		2.40 ± 0.25	100	FP/RF	18
299		2.16 ± 0.13	735	FP/RF	21
320	1,4-dioxane	2.09 ± 0.17 (42)	8.0–8.1	RR/DF/MS	this work
340	1,4-dioxane	1.23 ± 0.15 (23)	8.0–8.1	RR/DF/MS	this work
340	1,4-dioxane	1.19 ± 0.076 (24)	4.9–5.0	RR/DF/MS	this work
340	1,4-dioxane	0.986 ± 0.063 (24)	3.03–3.04	RR/DF/MS	this work
340	1,4-dioxane	0.727 ± 0.050 (28)	1.05–1.06	RR/DF/MS	this work

^a The number in parentheses represents the number of data points taken. Error bars are taken as 2σ . ^b He was used as a carrier bath gas. ^c Ar was used as a carrier bath gas. ^d DF, discharge flow; DP, direct photolysis; FP, flash photolysis; GC, gas chromatography; MS, mass spectrometry; RF, resonance fluorescence; RR, relative rate; SP, sensitized photolysis.

including calculations, are needed to scrutinize the cause of these differences.

Our kinetics results of the reaction of xylene with OH reveal an interesting trend of nonlinear temperature dependence at

240–340 K. Though it is difficult to pinpoint the temperature at which the *m*-xylene + OH reaction transitions from temperature independence to temperature dependence, it is clear that in all three reactions there is negative temperature dependence

TABLE 4: Rate Constants of the Reaction of *p*-Xylene with OH at 240–340 K

<i>T</i> (K)	reference compound	$k_{p\text{-xylene}} \times 10^{-11}$ ^a (cm ³ molecule ⁻¹ s ⁻¹)	<i>P</i> _{total} (Torr)	technique ^c	ref
240	1,4-dioxane	1.19 ± 0.08 (41)	8.0–8.1	RR/DF/MS	this work
260	1,4-dioxane	1.21 ± 0.09 (37)	8.0–8.1	RR/DF/MS	this work
277	1,4-dioxane	1.11 ± 0.07 (37)	8.0–8.1	RR/DF/MS	this work
296	propene	1.30 ± 0.20	735	FP/GC	9
296	cyclohexane	1.36	758	RR/DP/GC	13
297		1.22 ± 0.12	99.6	FP/RF	14
298	1,4-dioxane	1.19 ± 0.07 (118)	8.0–8.1 ^b	RR/DF/MS	this work
298		1.35 ± 0.14	99.8	FP/RF	16
298	<i>n</i> -hexane	1.36 ± 0.06	760	RR/DP/GC	17
298		1.53 ± 0.17	100	FP/RF	18
298		1.05 ± 0.06	200 ^b	FP/RF	19
300		1.3	760	DP/GC	15
304	<i>n</i> -butane	1.22 ± 0.25	758	RR/DP/UV–vis	12
320	1,4-dioxane	1.15 ± 0.09 (26)	8.0–8.1	RR/DF/MS	this work
320		1.38 ± 0.11	99.8	FP/RF	16
335		1.25 ± 0.13	99.8	FP/RF	16
340	1,4-dioxane	0.912 ± 0.072 (31)	8.0–8.1	RR/DF/MS	this work
340	1,4-dioxane	0.914 ± 0.062 (24)	4.93–4.94	RR/DF/MS	this work
340	1,4-dioxane	0.701 ± 0.056 (25)	3.07–3.09	RR/DF/MS	this work
340	1,4-dioxane	0.556 ± 0.039 (24)	8.0–8.1	RR/DF/MS	this work

^a The number in parentheses represents the number of data points taken. Error bars are taken as 2σ . ^b He was used as a carrier bath gas. ^c DF, discharge flow; DP, direct photolysis; FP, flash photolysis; GC, gas chromatography; MS, mass spectrometry; RF, resonance fluorescence; RR, relative rate; SP, sensitized photolysis; UV–vis, ultraviolet–visible spectroscopy.

at temperatures greater than 298 K. These observations suggest that the addition of the hydroxyl radical to the aromatic ring of the xylene molecule is a dominant process at lower temperatures, where an equilibrium is established between the reactant and the xylene–OH adduct.



At temperatures above 298 K, the addition mechanism is declining due to the shift of the equilibrium to the left of reaction 4, giving rise to a decrease in the rate constant for the xylene + OH reaction. Perry et al.¹⁸ and Nicovich et al.¹⁶ studied the temperature dependence of the rate constant of xylene + OH at 296–473 and 250–970 K, respectively, using the absolute rate technique. For the *o*- and *p*-xylene + OH at 298–320 K and *m*-xylene + OH at 250–320 K, Nicovich et al. reported little temperature dependence, which is in contrast with our findings. The reason for this discrepancy between the ranges is not well understood, and further investigations are needed. It is observed that in both Perry et al. and Nicovich et al.'s studies the decay of the OH radicals became nonlinear at around 340 K, which could also be attributed to the equilibrium nature of reaction 4. The complex, nonlinear temperature dependence of the reaction mechanism has also been observed in other similar systems such as reactions of OH with substituted benzenes and naphthalene.^{16,18,30} Nevertheless, the fact that the rate constant for the reaction of xylene with OH increases with temperature above 400 K^{16,18} suggests a domination of the abstraction mechanism of this chemical process at higher temperatures. Thus it is likely that our kinetic results at 298–340 K may reflect a transition of the reaction process from the addition mechanism to the abstraction mechanism, and the kinetics results below 298 K may signify a dominant addition mechanism for the reaction of xylene with the hydroxyl radicals.

In order to improve the confidence in using the $k_{\text{xylene+OH}}$ values determined in the present work at 8 Torr for atmospheric chemistry modeling, it is necessary to know if the observed negative temperature dependence of the $k_{\text{xylene+OH}}$ at 8 Torr

would reflect that the reaction is in the falloff region at high temperatures, since at higher temperatures additional third-body collisions may be necessary to remove the increased vibrational energy and stabilize the xylene–OH adducts. The falloff behavior has been observed with other OH + unsaturated VOC reactions at low pressure.³¹ We therefore conducted the pressure-dependent OH rate constant measurements at 340 K for *o*-, *m*-, and *p*-xylene in the present work, and the results are given in Tables 2–4 and summarized in Figure 3. Our kinetics results indicate that, at 340 K, the rate constant for the reaction of xylene with OH is always smaller than that at 298 K, which is expected for the above reason. However, the rate constants determined at 8 Torr at 340 K are not in the falloff region, since they are comparable to that at 5 Torr. As a result, the $k_{\text{xylene+OH}}$ values determined at 8 Torr and 340 K can still be regarded as high-pressure limits at this temperature. It should be pointed out that the high pressure limit study was conducted only at 298 and 340 K over 1–10 Torr in the present work, and it would be desirable to extend the investigation at temperatures lower than 298 K and pressures higher than 10 Torr for more accurate atmospheric chemistry modeling.

C. Atmospheric Lifetimes of Xylene + OH. Assuming that the only removal process of xylene from the atmosphere is via an oxidation reaction with the hydroxyl radical, the atmospheric lifetime of xylene can be evaluated using eq II. Previous literature has reported that the average atmospheric concentration of OH is $(8.1 \pm 0.9) \times 10^5$ molecules cm⁻³.²⁵ Consequently, the atmospheric lifetimes of *o*-, *m*-, and *p*-xylene are estimated to be about 29, 14, and 31 h, respectively, using our kinetics results at 277 K.

Conclusion

The kinetics of the reaction of OH with *o*-, *m*-, and *p*-xylene was studied at a pressure range of 1–10 Torr and temperature range of 240–340 K using the relative rate/discharge flow/mass spectrometry technique, with 1,4-dioxane + OH as a reference reaction. The room temperature rate constants for the reaction of OH with xylene exhibited prominent positive pressure dependence from 1 to 5 Torr, and the reactions were found to

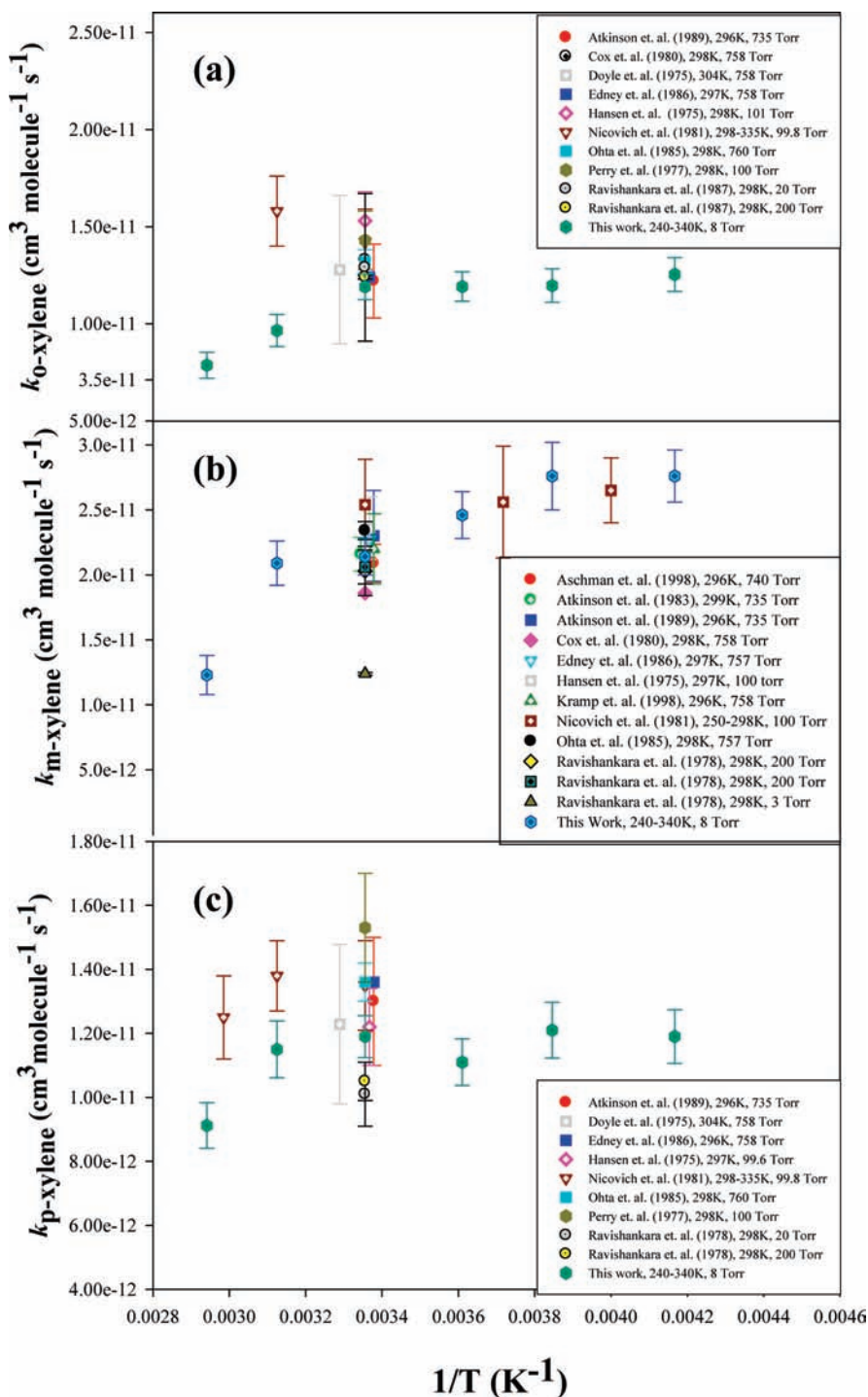


Figure 4. Temperature dependence of rate constants of (a) *o*-xylene + OH, (b) *m*-xylene + OH, and (c) *p*-xylene + OH at a range of 240–340 K and 8 Torr, along with available literature values.

reach a high-pressure limit at 8 Torr. The high pressure limit rate constants for *o*-, *m*-, and *p*-xylene at 298 K were determined to be $k_{o\text{-xylene}} = (1.19 \pm 0.07) \times 10^{-11} \text{ cm}^3 \text{ molecule}^{-1} \text{ s}^{-1}$, $k_{m\text{-xylene}} = (2.14 \pm 0.14) \times 10^{-11} \text{ cm}^3 \text{ molecule}^{-1} \text{ s}^{-1}$, and $k_{p\text{-xylene}} = (1.19 \pm 0.07) \times 10^{-11} \text{ cm}^3 \text{ molecule}^{-1} \text{ s}^{-1}$, respectively, which are in good agreement with most literature values. The temperature dependence study results indicated that the rate constants of OH + xylene depend negatively on temperature at 298–340 K. The reaction of OH with xylene may proceed with addition of the OH radical to the benzene ring at room temperature and below, with an equilibrium established between the reactants and the xylene–OH adduct. At 298–340 K the

equilibrium is shifted toward the reactants, resulting in a negative temperature dependence of the rate constant, and it may also reflect a transition of the reaction process from the addition mechanism to the abstraction mechanism. Finally, on the basis of our kinetic results at 277 K, the atmospheric lifetimes of *o*-, *m*-, and *p*-xylene are estimated to be ca. 29, 14, and 31 h, respectively, assuming that the primary removal process of xylene from the atmosphere is via reaction with OH.

Acknowledgment. This work is supported in part by the National Science Foundation (NSF ATM-0533574; REU NSF CHE 0649087).

References and Notes

- (1) Gail, S.; Dagaut, P. *Combust. Flame* **2005**, *141*, 281–297.
- (2) Celebi, U.; Vardar, N. *Atmos. Environ.* **2008**, *42*, 5685–5695.
- (3) Baker, A.; Beyersdorf, A.; Doezema, L.; Katzenstein, A.; Meinardi, S.; Simpson, I.; Blake, D.; Rowland, S. *Atmos. Environ.* **2008**, *42*, 170–182.
- (4) Jia, C.; Batterman, S.; Godwin, C. *Atmos. Environ.* **2008**, *42*, 2083–2100.
- (5) McCarthy, M.; Hafner, H.; Chinkin, L.; Charrier, J. *Atmos. Environ.* **2007**, *41*, 7180–7194.
- (6) Environmental Protection Agency. Toxicological Review of Xylenes. <http://www.epa.gov/ncea/iris/toxreviews/0270-tr.pdf> (accessed 2008).
- (7) Finlayson-Pitt, B.; Pitts, J. *Chemistry of the Upper and Lower Atmosphere*; Academic Press: San Diego, CA, 2000.
- (8) Song, C.; Na, K.; Warren, B.; Malloy, Q.; Cocker, D. *Environ. Sci. Technol.* **2007**, *41*, 7403–7408.
- (9) Atkinson, R.; Aschmann, S. M. *Int. J. Chem. Kinet.* **1989**, *21*, 355.
- (10) Anderson, R. S.; Czuba, E.; Ernst, D.; Huang, L.; Thompson, A. E.; Rudolph, J. *J. Phys. Chem. A* **2003**, *107*, 6191–6199.
- (11) Cox, R.; Derwent, R.; Williams, M. *Environ. Sci. Technol.* **1980**, *14*, 57–61.
- (12) Doyle, G.; Lloyd, A.; Darnall, K. R.; Winer, A.; Pitts, J. *Environ. Sci. Technol.* **1975**, *9*, 237–241.
- (13) Edney, E. O.; Kleindienst, T. E.; Corse, E. W. *Int. J. Chem. Kinet.* **1986**, *18*, 1355–1371.
- (14) Hansen, D. A.; Atkinson, R.; Pitts, J. N., Jr. *J. Phys. Chem.* **1975**, *79*, 1763.
- (15) Klopffer, W. W.; Frank, R.; Hohl, E. G.; Haag, F. *Chem. Ztg.* **1986**, *110*, 57–62.
- (16) Nicovich, J. M.; Thompson, R. L.; Ravishankara, A. R. *J. Phys. Chem.* **1981**, *85*, 2913.
- (17) Ohta, T.; Ohya, T. *Bull. Chem. Soc. Jpn.* **1985**, *58*, 3029–3030.
- (18) Perry, R. A.; Atkinson, R.; Pitts, J. N., Jr. *J. Phys. Chem.* **1977**, *81*, 296.
- (19) Ravishankara, A. R.; Wagner, S.; Fischer, S.; Smith, G.; Schiff, R.; Watson, R. T.; Tesi, G.; Davis, D. D. *Int. J. Chem. Kinet.* **1978**, *10*, 783.
- (20) Aschmann, S. M.; Atkinson, R. *Int. J. Chem. Kinet.* **1998**, *30*, 533–40.
- (21) Atkinson, R.; Aschmann, S. M.; Carter, W. P. L. *Int. J. Chem. Kinet.* **1983**, *15*, 37–50.
- (22) Kramp, F.; Paulson, S. E. *J. Phys. Chem. A* **1998**, *102*, 2685.
- (23) Li, Z. *Chem. Phys. Lett.* **2004**, *383*, 592–600.
- (24) Dagaut, P.; Liu, R.; Wallington, T. J. *J. Phys. Chem.* **1990**, *94*, 1881.
- (25) Prinn, P.; Cunnold, D.; Simmonds, P.; Alyea, F.; Bold, R.; Crawford, A.; Fraser, P.; Gutzler, D.; Hartley, D.; Rosen, R.; Rasmussen, R. *J. Geophys. Res.* **1992**, *97*, 2445.
- (26) Li, Z.; Nguyen, P.; de Leon, M. F.; Wang, J. H.; Han, K.; He, G. Z. *J. Phys. Chem. A* **2006**, *110*, 2698–2708.
- (27) Li, Z.; Pirasteh, A. *Int. J. Chem. Kinet.* **2006**, *38*, 386–398.
- (28) Li, Z.; Singh, S.; Woodward, W.; Dang, L. *J. Phys. Chem. A* **2006**, *110*, 12150–12157.
- (29) Li, Z.; Singh, S. *J. Phys. Chem. A* **2007**, *111*, 11843–11851.
- (30) Lorenz, K.; Zellner, R. *Ber. Bunsenges. Phys. Chem.* **1983**, *87*, 629–636.
- (31) Chuong, B.; Davis, M.; Edwards, M.; Stevens, P. S. *Int. J. Chem. Kinet.* **2002**, *34*, 300–308.

JP905074J